八、附件及參考資料

附件 1 美國深層地熱 FORGE 計畫猶他場址現況

THE UTAH FRONTIER OBSERVATORY FOR GEOTHERMAL RESEARCH (FORGE): A LABORATORY FOR EGS DEVELOPMENT

Joe Moore[1], Rick Allis[2], Kristine Pankow[3], Stuart Simmons[1], John McLennan[1], Philip Wannamaker[1], William Rickard[4], Robert Podgorney[5]

[1]Energy and Geoscience Institute, University of Utah, Salt Lake City, Utah

[2] Utah Geological Survey, Salt Lake City, Utah

[3]University of Utah Seismograph Stations, University of Utah, UT 84112

[4] Geothermal Research Group, Palm Desert, California

[5]Idaho National Laboratory, Idaho Falls, Idaho

jmoore@eri.utah.edu

Keywords: *FORGE, Milford, Utah, Enhanced Geothermal Systems*

ABSTRACT

The U.S. Department of Energy is sponsoring the FORGE (Frontier Observatory for Research in Geothermal Energy) initiative to bring Enhanced Geothermal System (EGS) development to commercial viability and visibility. The project will create a controlled environment where EGS technologies can be developed and tested.

The Utah FORGE site, one of two sites being considered, is located in central Utah, 350 km south of Salt Lake City. Since the 1970s, more than 100 wells, the deepest to 3.8 km, have been drilled in the vicinity of the site. Well logs, detailed geologic mapping, geophysical surveys and seismic data provide information on temperatures, thermal gradients, rock types, and in-situ stresses. High angle, northeast-trending faults that formed during east-west extension offset the alluvium and recent sinter deposits but these do not extend into the FORGE site. Thirty years of monitoring indicates that natural seismicity surrounding the FORGE site is low. The data indicate the site is underlain by large volumes of Tertiary granite and Precambrian gneiss with temperatures from 175–225°C at depths of 2 to 4 km. Fault orientations, borehole breakouts, and earthquake solutions indicate the maximum horizontal stress is NNE-SSW.

The project is being conducted in multiple phases. Phases 1 and 2A included project planning and review of potential environmental and cultural constraints. None that could adversely affect the project were identified. Phase 2B includes drilling a 2.1 km deep well to determine in-situ stresses, permeability, lithology and temperature within the thermal reservoir. Preliminary results from this well will be presented. At the conclusion of Phase 2B, a final site for the FORGE laboratory will be selected. In subsequent phases, the supporting infrastructure will be built and wells for injection and production will be drilled, stimulated and tested.

1. INTRODUCTION

The first Enhanced Geothermal Systems (EGS) demonstrations were conducted at Fenton Hill, New Mexico in the late 1970s and early 1980s. Although the Fenton Hill project demonstrated the potential of EGS development, no EGS project has yet reached large-scale commercial levels of production. The goal of the U.S. Department of Energy's Frontier Observatory for Research in Geothermal Research (FORGE) program is to develop the techniques required for creating, sustaining and monitoring EGS reservoirs for commercial development.

The FORGE program consists of three phases. Phase 1 involved desktop studies of existing data at five sites. At the conclusion of Phase 1, two sites were selected, the University of Utah's Milford, Utah site and Sandia National Laboratories Fallon, Nevada site. During Phase 2, a 2134 m well MU-ESW1 will be drilled at the Utah FORGE site to obtain direct measurements on temperature, stress, rock type and permeability in the granitic reservoir rocks. Compliance with the National Environmental Policy Act will be demonstrated and a Seismic Hazard Program will be prepared. The U.S. DOE will select a final site for FORGE in mid-2018. Essential Phase 3 activities include the creation and monitoring of the EGS reservoir, characterization and modeling of the heat exchange potential of the reservoir through the stimulated fracture network, and monitoring of microseismicity. The ultimate goal of the FORGE project is to demonstrate to the public, stakeholders and the energy industry that EGS technologies have the potential to contribute significantly to power generation in the future.

2. THE UTAH FORGE SITE

The Utah FORGE site is located 350 km south of Salt Lake City and 16 km north of Milford, a small community with a population of 1400 (Fig. 1). The FORGE site is unpopulated and covers an area of about 5 km^2. It is situated within Utah's Renewable Energy Corridor adjacent to a 306 MWe wind farm, a 240 MWe solar field and PacifiCorp Energy's 38 MWe Blundell geothermal plant at Roosevelt Hot Springs. Cyrq Energy's 10.5 MWe geothermal field at Thermo and a biogas facility are located approximately the same distance south of Milford.

Considerable supporting infrastructure exists near the site. Milford has motel accommodations, a supermarket, hardware store, and a hospital. Beaver, a larger population center, is located 56 km from Milford adjacent to I-15, a major interstate. The Union Pacific Railroad passes through Milford, offering the possibility of shipping heavy equipment by rail and then by truck to the FORGE site. The Milford Municipal Airport, located a few kilometers north of Milford, has a 1524 m long sealed runway that can accommodate piston or turboprop, single- or twin-engine planes.

Proceedings 39th New Zealand Geothermal Workshop
22 - 24 November 2017
Rotorua, New Zealand

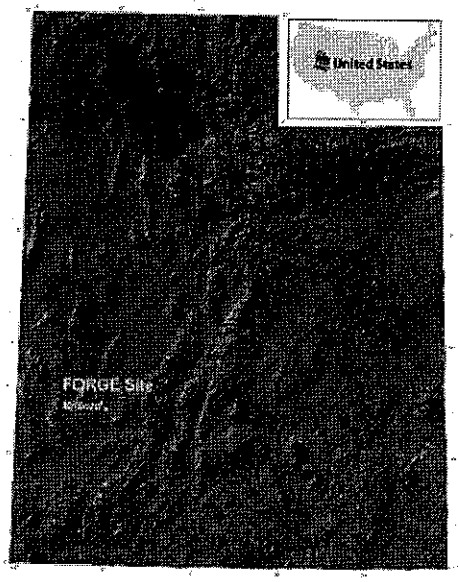

Figure 1: Location map.

The area around the FORGE site has been the focus of numerous geoscientific studies over the last 40 years, starting with intensive geothermal exploration during the late 1970s (Fig. 2). Geological mapping, gravity and magnetotelluric surveys, and the drilling, logging, and sampling of 80 shallow (<500 m) and 20 deep (> 500 m) wells, including Acord-1, a 3.8 km deep well in the middle of north Milford Valley, 3 km west of the FORGE drill site, were conducted. Wells 9-1 and 82-33 were drilled west and north of the Roosevelt Hot Springs geothermal system as part of the geothermal development program.

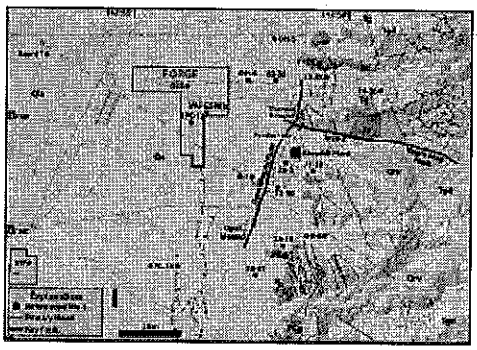

Figure 2: Geologic map of the FORGE site and surrounding area, Milford, Utah from Nielson et al., 1986. For clarity, only a few of the many wells are shown. Abbreviations for map units: Qa=Quaternary alluvium; Qrv=Quaternary rhyolite; Tgd=Tertiary granodiorite; Tg=Tertiary granite dike; Ts=Tertiary syenite; PCg=Precambrian gneiss.

The FORGE well site is situated centrally between these three, deep, non-productive wells, all of which display conductive thermal gradients and temperatures of more than 175°C at less than 3 km depth. The data from these wells demonstrate the FORGE site is outside the boundaries of any existing hydrothermal system and that the required reservoir criteria of temperature (175°-225°C), rock type (crystalline rock) and depth (1.5-4 km) established by the U.S. DOE exist at the site. The availability of non-potable water, the lack of environmental issues, the local infrastructure, and the extensive suite of existing scientific and well data are additional supporting considerations.

3. GEOLOGY

The FORGE site is located on a gently sloping alluvial plane on the west flank of the Mineral Mountains. The geology of the Mineral Mountains east of the FORGE site is shown in Figure 2. Here the geology is composed of Precambrian gneiss, Tertiary plutons and Quaternary rhyolite (Kirby, et al., 2012). Isotopic dating indicates metamorphism of the Precambrian rocks occurred ~1720 Ma (Aleinikoff et al., 1987).

The Tertiary plutonic rocks include diorite, granodiorite, quartz monzonite, syenite, and granite. Their subsurface distributions are known primarily from detailed investigations of four wells, 14-2, 52-21, 9-1, and Acord-1 (Glen and Hulen, 1978; Glenn et al., 1980; Sweeny, 1980; Welsh, 1980; Nielson et al., 1986; Coleman and Walker, 1992; Coleman et al., 1997; Hintze and Davis, 2003). U-Pb zircon dating indicates development of the plutonic complex that began with the emplacement of (hornblende) diorite at 25.4 Ma (Aleinikoff et al., 1987); younger plutonic rocks were emplaced at ~18 Ma and 11 to 8 Ma (Nielson et al., 1986; Coleman and Walker, 1992; Walker et al., 1997).

The youngest intrusions produced <1 Ma rhyolites that form domes along the crest of the range. Temperatures 250°C in the Roosevelt Hot Springs reservoir and to the west in Acord-1 suggest the presence of a still cooling magma chamber in the shallow crust extending westward from the crest of the range.

The Tertiary and Quaternary basin fill in the Milford Valley consists dominantly of alluvial and lacustrine deposits that contain interbedded sand, silt, gravel, and clay (Hintze and Davis, 2003). In Acord-1, nearly 3 km of unconsolidated basin fill was encountered above the crystalline basement rocks (Fig. 2). Minor thicknesses of Tertiary ash-flow tuffs, probably Miocene in age, are present but have not been found in wells drilled at Roosevelt Hot Springs. At the FORGE site, the basin fill is 637 m thick.

Paleozoic and Mesozoic sedimentary sequences are exposed at the northern and southern parts of the Mineral Mountains. These sedimentary rocks are major components of the regional stratigraphy but were not encountered in any of the deep wells (Nielson et al., 1986).

4. STRUCTURAL RELATIONSHIPS

The structural setting of the FORGE site reflects the effects of two distinct tectonic events; late Mesozoic to early Cenozoic compression during the Sevier orogeny and middle Tertiary to Recent extension. The Sevier orogeny produced large-scale low-angle thrust faults found in the surrounding mountain ranges (e.g., Hintze and Davis, 2003), but the effects of this orogeny near the FORGE site are poorly understood.

The younger faulting episode is related to ongoing east-west Basin and Range extension, which dates back to at least ~17

Ma. This extension has produced predominantly north-south trending fault zones (e.g., Hintze and Davis, 2003; Dickinson, 2006). The most prominent of the Basin and Range structures shown in Figure 2 is the Opal Mound Fault), which dips steeply to the east and offsets surficial deposits of alluvium and silica sinter, with a total down-dip displacement of at least 15 m (Nielson et al., 1986). This fault separates the convective thermal regime of the Roosevelt Hot Springs geothermal system from the conductive thermal regime to the west, beneath the FORGE site.

South of the Opal Mound Fault, north-south trending faults form a series of short, narrow grabens and horsts (Nielson et al., 1986). These faults die out to the north as the FORGE site is approached.

The Negro Mag fault is another major steeply dipping fault, but it trends east-west (Fig. 2). The fault cuts across the Mineral Mountains for ~6 km, however the direction and amount of displacement are unknown due to the absence of markers within the plutonic rocks (Nielson et al., 1986). An east-west trending structure, 2 km south of Negro Mag fault, was the site of seismicity in the late 1970s (Zandt et al., 1982; Nielson et al., 1986). Both the Negro Mag and Opal Mound faults appear to terminate at their intersection. These east-west faults may reflect regional arc-parallel structures, formed as Eocene-Oligocene magmatism migrate southward migrating and/or Proterozoic structures in the deep-seated basement (e.g., Dickinson, 2006; Wannamaker et al., 2015).

The direction of S_{Hmax} in the vicinity of the Milford FORGE (Fig. 3) site is constrained by: 1) borehole breakouts in 52-21; 2) image logs in 14-2 (Keys, 1979); 3) the attitudes of joints and dikes (Yusas and Bruhn, 1979); and 4) focal mechanisms of seismic events; (e.g., Whidden and Pankow, 2012); These data all indicate a consistent maximum horizontal compressive stress, S_{Hmax}, primarily directed N-S (170-180°) to NNE-SSW (035°).

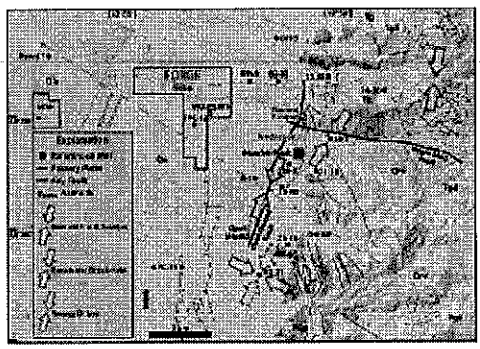

Figure 3. Summary of S_{Hmax} orientations based on normal fault scarps, borehole breakouts and young dikes. Stress data compiled by Davatzes (2016, written comm.)

Mechanical testing of core samples of Precambrian gneiss from 52-21 indicates the rock is very strong, with very low porosity and permeability. The compressive strength was measured at three separate confining pressures, 0, 2800, and 8000 psi, giving average values of 2.8×10^4, 6.0×10^4, and 9.0×10^4 psi, respectively. The porosity is 0.13% and the permeability was measured at 0.3 microdarcies. These data imply that permeability enhancement within the FORGE reservoir will rely on hydroshearing of existing fractures and not the creation of new fractures.

Detailed fracture mapping of the plutonic rocks in the Mineral Mountains has identified three fracture sets (Bartley, 2017, written comm.): steep E-W fractures; gently west dipping fractures; and steep N-NNE striking fractures. Direct information on the behavior of these fractures will be obtained after MU-ESW1 (Fig. 2) is completed and a minifrac is conducted in the reservoir rocks.

5. THERMAL STRUCTURE

More than 100 shallow and deep wells provide temperature data surrounding the FORGE site. Wells located between the central Milford Valley and the Opal Mound fault show that the heat flow ranges from 120 to 200 mW/m^2. In the vicinity of the FORGE site (e.g. TPC-12 in Fig. 4), the heat flow is in the range 180 ± 40 mW/m^2. To the east; in 9-1 and 82-33, the heat flows are significantly higher at depths less than about 500 m. However, temperatures in these wells at shallow depths are affected by outflow from the Roosevelt Hot Springs geothermal system. Although near-surface gradients exceed 150°C/km and heat flows range from 300 to >1000 mW/m^2, (for example, well RHS-335; Fig. 4). These temperature gradients cannot be extrapolated much below 500 m depth, and when RHS-335 is compared to 9-1, the gradients are clearly decreasing with increasing depth (Fig. 4).

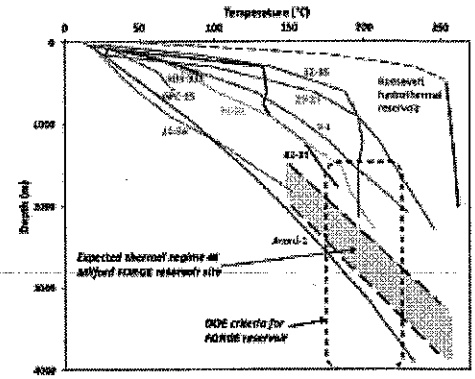

Figure 4. Temperature and pressure profiles in wells surrounding the FORGE site. The dashed rectangle shows conditions required by the U.S. DOE. See Figure 2 for well locations. Productive wells tapping the Roosevelt Hot Springs geothermal system display convective thermal gradients. These wells lie east of the Opal Mound fault. The three deep wells surrounding the FORGE site, Acord-1, 82-33 and 9-1, display conductive gradients

East of the Opal Mound fault, many of the shallow temperature profiles exhibit boiling-point-for- depth profiles, indicative of hydrothermal upflow. Here, in contrast to the conductive thermal gradients west of the Opal Mound fault, the thermal gradients are convective and the temperature profiles are controlled by steam-water saturation conditions and hydrostatic pressure gradients.

Integration of all temperature gradient data shows that a large area of anomalously high conductive heat flow, covering about 100 km^2, surrounds the FORGE site (Fig. 5). The total volume of crystalline basement rock having temperatures

>175°C down to 4 km depth is more than 100 km³. The Opal Mound fault forms the eastern boundary this thermal regime and, as discussed below, marks the transition to the Roosevelt Hot Springs where convective heat flow prevails and covers a much smaller area of ~10 km².

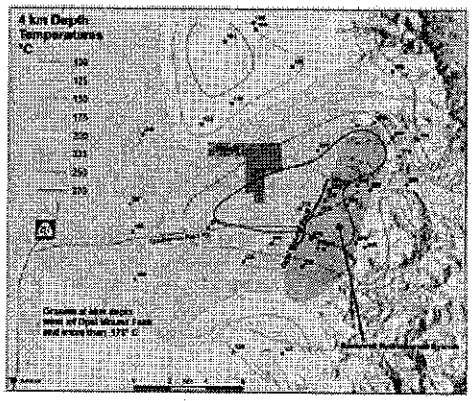

Figure 5. Contours of temperature at 4 km depth derived from observations in the deep wells and geotherms fitted to thermal gradient wells. The stipple area indicates where the granite is hotter than the minimum reservoir temperature of 175°C. The red shading shows the extent of the Roosevelt Hot Springs geothermal system.

Prior to the start of production at Roosevelt Hot Springs in 1984, deep wells east of the Opal Mound fault had a uniform pressure profile consistent with hot water having a density of 800 kg/m³ (Allis and Larsen, 2012; Fig. 6). The one deep well west of the Opal Mound fault, 82-33, had a pressure profile consistent with cold water with a density of 1000 kg/m³, about 30 bars lower than wells on the east side of the Opal Mound fault in the Roosevelt Hot Springs geothermal system (Faulder, 1994). Other wells west of the Opal Mound fault plot on the same pressure gradient as 82-33. These well data indicate the existence of a major pressure boundary, which coincides with the Opal Mound fault. Well 9-1 is located on that boundary and is unproductive, and it is used as a monitoring well. These data imply the presence of two distinct pressure regimes across the Opal Mound fault (Allis et al., 2016). The FORGE site lies to the west of this barrier. At a depth of 2.5 km depth, the pressure within the FORGE reservoir is expected be at 228 bars (3300 psi).

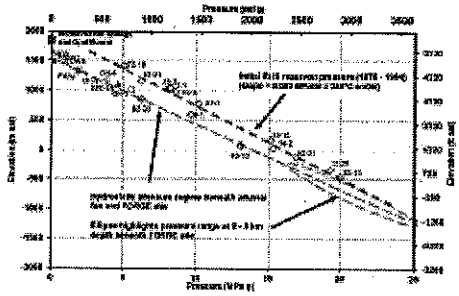

Figure. 6. Pressure profiles in wells surrounding the FORGE site. Wells within the Roosevelt Hot Springs geothermal system display a hydrostatic pressure head that is 30 bars higher than wells on the west side of the Opal Mound fault.

6. GEOMETRY OF THE BASEMENT ROCKS

Gravity and well data constrain the depth to the crystalline rocks west of the Mineral Mountains (Fig. 7). The central part of the Milford Basin, beneath Acord-1, is steep walled and V-shaped. The basin axis is oriented north-south, perpendicular to Basin and Range extension. Outward and upward, the basement contact flattens to form a gently dipping surface that extends beneath the FORGE site, where the depth to the crystalline basement ranges from over 1000 m on the western side to about 600 m on the eastern side. Buried faults near the deepest part of the basin are inferred from the gravity profile and westward thickening of the basin fill (Allis et al., 2016; Hardwick et al., 2016).

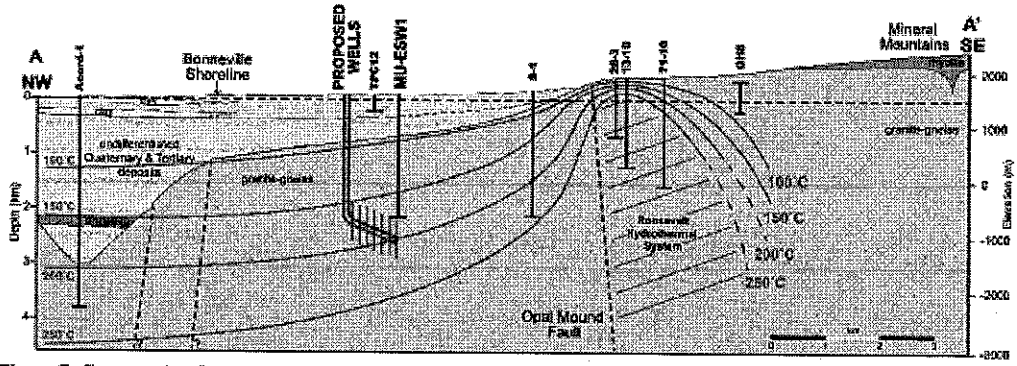

Figure 7. Cross section A-A' from Figure 2, showing the top of the crystalline basement rocks in the Milford Basin in the vicinity of the FORGE site. Precambrian gneiss and Tertiary plutonic rocks are undifferentiated. The Roosevelt Hot Springs hydrothermal system lies east of the Opal Mound fault. Isotherms are interpreted from well measurements. The figure shows the proposed FORGE injection and production wells and the vertical 2134 m deep test well currently being drilled.

7. MICROSEISMICITY

Seismicity has been monitored in the area around the FORGE site since 1981 by the University of Utah Seismograph Stations (UUSS) (Pankow et al., 2017). Analysis of the UUSS catalog shows that seismic events near the Utah FORGE site tend to cluster in three areas; one near Milford, the second 10 km northwest of Milford and the third northeast of Milford, east and southeast of the FORGE site (Fig. 8). The events northwest of Milford occur only during daylight hours and are characterized by small magnitudes (M=0.49 to 2.05), shallow depths (above 2.5 km below sea level), and highly correlated waveforms implying a similar location and source mechanism. These events are interpreted as the result of quarry blasts, not tectonic earthquakes (box labeled Quarry; Fig.8).

Seismic events located near Milford (box labeled Airport, Fig. 8) are not far from a 1908 M=4.1 event. The magnitudes of these tectonic events range from 0.46 to 3.87. Based on the moment tensor from an M=3.8 earthquake (depth 6 km), the direction of minimum horizontal stress (T-axis, or S_{hmin}) is NW-SE (Whidden and Pankow, 2012), close to the extension direction inferred for the Milford Basin although the focal mechanism for this event is strike-slip.

Northeast of Milford, seismicity occurs primarily within the box labeled Mineral Mountains (Fig. 8) east of the FORGE site. In November, 2016, the seismic network was upgraded with the installation of five broadband seismometers in order to monitor seismicity under the FORGE site. These seismometers allow detection of seismic events with magnitudes <0. Significantly, no evidence of seismic activity under the Utah FORGE site has been detected by the newly installed network.

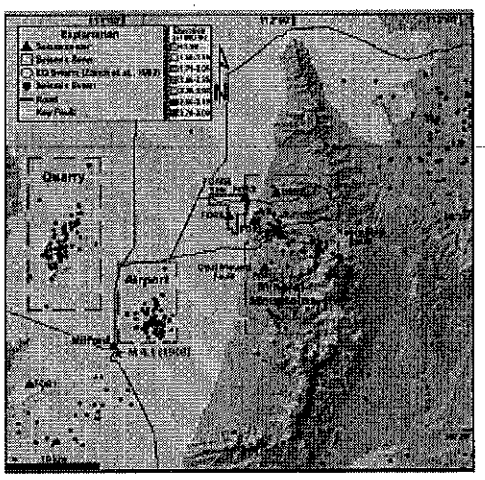

Figure 8. Locations of seismic events in the region surrounding the FORGE site (red outline) (Pankow et al., 2017). Black circles are seismic events occurring between 1981- 2016. The red star marks the location of the 1908 M 4.1 Milford earthquake. Brown dashed boxes show the locations of seismic source zones. The black square near the 1908 seismic event is the town of Milford. Purple triangles are seismic stations. The Opal Mound and Negro Mag faults are shown in yellow. The blue polygon is the area of the earthquake swarm defined by Zandt et al. (1982).

Faults within the alluvium provide a record of seismicity during Quaternary time. Faults are present in the alluvium south of the FORGE site but do not continue northward into the site. Although the deposits have not been dated directly, the least dissected alluvium within the FORGE site is cut by the Pleistocene Lake Bonneville shoreline. This suggests the deposits are more than ~18,000 years old (Kleber et al., 2017).

Potter et al., (2017) examined the relationship between microseismicity and injection at the nearby Blundell geothermal power plant but found none (Fig. 9). The lack of any correlation with injection suggests injection at the FORGE site, into the same reservoir rocks, will not lead to significant induced seismicity.

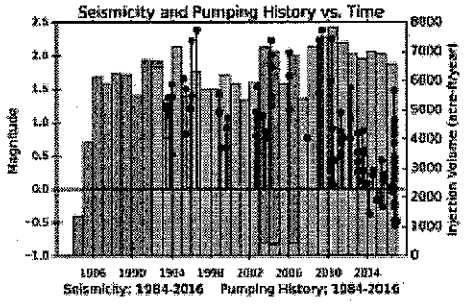

Figure 9. Time-magnitude histories of seismic events, shown as blue circles, located northeast of Milford and east of the FORGE site. No seismic events have been located within the FORGE footprint. Green bars represent the Blundell power plant injection history; cross hatched regions calculated based on the plants power production. No visible correlation is apparent between the seismic events and the volume of fluids injected.

8. CONCLUSION

The Milford FORGE site is ideally suited for the development and testing of technologies that can be used to create and sustain EGS reservoirs. The FORGE reservoir will be developed in weakly altered Tertiary granite and Precambrian gneiss at a depth below about 1980 m. The geology and thermal structure of the region surrounding the site is well characterized as a result of geological mapping, geophysical surveys and the drilling, logging, and sampling of nearly 100 wells, since the 1970s. Additional direct information on rock types, fracture abundances and orientations, temperature, permeability, and stress characteristics at the site will be obtained from measurements in a 2134 m vertical well currently being drilled.

The FORGE site is separated from the nearby Roosevelt Hot Springs geothermal system by the north-south trending Opal Mound fault that has formed in response to ongoing east-west Basin and Range extension. Temperatures within the geothermal system are close to 250°C. Convective thermal gradients characterize wells east of the Opal Mound fault whereas conductive thermal gradients characterize wells surrounding the FORGE site west of the Opal Mound fault.

Pre-production pressure profiles of deep wells in the geothermal system display a hydrostatic pressure head that is 30 bars higher than wells on the west side of the Opal Mound

fault. This pressure difference requires the presence of two distinct pressure regimes, with high-permeability rock associated with the hydrothermal system to the east, and relatively impermeable rock to the west beneath the FORGE site.

The existing geoscientific data demonstrate the FORGE site is outside the boundaries of any existing hydrothermal system and that the required reservoir criteria of temperature (175°-225°C), rock type (crystalline rock) and depth (1.5-4 km) established by the U.S. DOE for EGS development exist at the site. The low risk of seismic activity and impact to the environment, a well-developed local infrastructure, the absence of potable groundwater, endangered fauna or flora and a welcoming community, are additional positive attributes of the site.

ACKNOWLEDGEMENTS

Funding for this work was provided by U.S. DOE grant DE-EE0007080 "Enhanced Geothermal System Concept Testing and Development at the Milford City, Utah FORGE Site". We thank the many stakeholders who are supporting this project, including Smithfield, Utah School and Institutional Trust Lands Administration, Beaver County and PacifiCorp. The Bureau of Land Management and the Utah State Engineer's Office have been very helpful in guiding the project through the permitting processes. Mark Gwynn and Gosia Skowron assisted in the preparation of the figures and manuscript. The help is greatly appreciated.

REFERENCES

Allis R. G. and Larsen, G., 2012, Roosevelt Hot Springs Geothermal field, Utah—reservoir response after more than 25 years of power production. Proceedings. 37th Workshop on Geothermal Reservoir Engineering, Stanford University, Stanford, CA.

Allis, R.G., Moore, J.N., Davatzes, N., Gwynn, M., Hardwick, C., Kirby, S., Pankow, K., Potter, S., and Simmons, S.F., 2016, EGS Concept Testing and Development at the Milford, Utah FORGE Site. Proceedings, 41st Workshop on Geothermal Reservoir Engineering, Stanford University, Stanford, CA.

Aleinikoff, J.N., Nielson, D.L., Hedge, C.E., and Evans, S.H., 1987, Geochronology of Precambrian and Tertiary rocks in the Mineral Mountains, south-central Utah. US Geological Survey Bulletin, 1622, p. 1-12.

Coleman, D.S., and Walker, J.D, 1992, Evidence for the generation of juvenile granitic crust during continental extension, Mineral Mountains batholith, Utah. Journal of Geophysical Research, 97, pp. 11011-11024.

Coleman, D.S., Bartley, J.M., Walker, J.D., Price, D.E., and Friedrich, A.M., 1997, Extensional faulting, footwall deformation and plutonism in the Mineral Mountains, southern Sevier Desert, in Link, P.K., and Kowallis, B.J., editors, Mesozoic to recent geology of Utah: Brigham Young University Geology Studies, v. 42, part 2, pp. 203–233.

Dickinson, W. R., 2006, Geotectonic evolutions of the Great Basin. Geosphere, 2, pp.353-368.

Faulder, D.D., 1994, Long-term flow test #1, Roosevelt Hot Springs, Utah. Transactions, Geothermal Resources Council Transactions, 18, pp. 583-590.

Glenn, W.E., and Hulen, J. B., 1979, Interpretation of well log data from four drill holes at Roosevelt Hot Springs KGRA. DOE Earth Science Laboratory Report, University of Utah, pp. 74.

Glenn, W.E., Hulen, J. B., and Nielson, D.L., 1980, A comprehensive study of LASL well C/T-2 Roosevelt Hot Springs KGRA, Utah, and applications to geothermal well logging. Los Alamos Scientific Laboratory Report, LA-8686-MS, pp 175.

Hardwick C.L., Gwynn, M., Allis, R., Wannamaker, P., and Moore, J., 2016, Geophysical Signatures of the Milford, Utah FORGE Site. Proceedings, 41st Workshop on Geothermal Reservoir Engineering, Stanford University, Stanford, CA.

Hintze, L. F., and Davis, F. D., 2003, Geology of Millard County, Utah. UGS Bulletin, 133, pp. 305.

Keys, W. S., 1979, Borehole geophysics in igneous and metamorphic rocks, in Society of Professional Well Log Analysts Annual Logging Symposium, 20th, Tulsa, Okla., 1979, Tulsa, Okla., Transactions: Houston, Society of Professional Well Log Analysts, pp. 001-0026.

Kirby, S., 2012, Geologic and hydrologic characterization of regional nongeothermal groundwater resources in the Cove Fort area, Millard and Beaver Counties, Utah. Utah Geological Survey Special Study, 140, 46 p.

Kleber, E., Hiscock, A., Kirby, S., Allis, R., Quirk, B., 2017, Assessment of Quaternary Faulting near the Utah FORGE Site from High Resolution Topographic Data, Proceedings Geothermal Resources Council, in press.

Nielson, D. L., Evans, S.H., and Sibbett, B.S., 1986, Magmatic, structural, and hydrothermal evolution of the Mineral Mountains intrusive complex, Utah, Geological Society of America Bulletin 97, pp. 765-777.

Pankow, K., L. Pankow, Potter, S., Zhang, H. and Moore J., 2017, Local seismic monitoring at the Milford, Utah FORGE site: Proceedings Geothermal Resources Council, in press.

Potter, S., Pankow, K., Moore, J., Allis, R., 2017, Seismicity in the Mineral Mountains, Utah and the Possible Association with the Roosevelt Hot Springs Geothermal System. Seismological Society of America poster presentation.

Sweeney, M.J., 1980, McCulloch Acord 1-26, Roosevelt Hot Springs Area, Beaver Co., Utah. Unpublished petrography.

Wannamaker, P. E., Moore, J. N., Pankow, K. L., Simmons, S.F., Nash, G. D., Maris, V., Batchelor, C., and Hardwick, C. L., 2015, Play Fairway Analysis of the Eastern Great Basin Extensional Regime, Utah: Preliminary Indications. Proceedings Geothermal Resources Council 39, pp. 793-804.

Welsh, J. E., 1980, McCulloch Acord 1-26, Roosevelt Hot Springs Area, Beaver Co., Utah. Unpublished petrography.

Whidden K.M. and K.R. Pankow, 2012, A catalog of Regional Moment Tensors in Utah from 1998 to 2011, Seismological Research Letters, v 83, pp. 775-783. doi: 10.1785/0220120046

Yunas, M.R. and R.L. Bruhn, 1979, Structural Fabric and in-situ stress analysis of the Roosevelt Hot Springs KGRA; Topical Report 78-1701f.a.6.5.1, DE-AC07-78ET28392, Department of Geology and Geophysics, University of Utah, 62 p.

Zandt, G., McPherson, L., Schaff, S., and Olsen, S., 1982, Seismic baseline and induction studies: Roosevelt Hot Springs, Utah, and Raft River, Idaho. U.S. Dept. of Energy Report DOE 01821-T1, 58 p.

附件 2 研討會議程及內容

NZGW 2017 Programme

Wednesday 22 November 2017				
08:35	Welcome and Opening Room: Mokoia Room			
09:20	Keynote 1 - Rupert Sutherland Room: [illegible]			
10:00	Morning Tea			
	Session 1.1: Modelling Room: Mokoia Room	**Session 1.2: Geology** Room: Millennium 3	**Session 1.3: Environment** Room: Millennium 1	**Session 1.4: Other Themes** Room: Millennium 2
10:20	3: TARGETING LOCALISED UPWELLINGS WITH A NEW MULTIPHYSICS SIMULATOR (Tung)	6: THE HEYUAN FAULT, SOUTH CHINA: A DEEP GEOTHERMAL PROSPECT – THE ROLE OF FAULT INTERSECTION RELATIONSHIPS AND FLUID FLOW (Tannock)	30: ABSTRACT 1: ROTORUA GEOTHERMAL SYSTEM: CURRENT AND FUTURE MANAGEMENT (Doorman)	28: GEOTHERMAL TOURISM IN NZ: BORROWING FROM INTERNATIONAL EXAMPLES (Blair)
10:40	4: NEXT GENERATION RESERVOIR ENGINEERING FOR A GEOTHERMAL FUTURE (Regenauer-Lieb)	11: POST-DEPOSITIONAL ALTERATION OF SILICEOUS SINTER NEAR OLD FAITHFUL GEYSER, YELLOWSTONE NATIONAL PARK, USA. (Lynne)	31: ABSTRACT 2: ROTORUA GEOTHERMAL FILED - METHOD TO MEASURE HEAT AND FLUID USE (Barber)	42: VALUING USES OF THE WAIKATO AND BAY OF PLENTY GEOTHERMAL RESOURCES (Luketina)
11:00	56: GEOTHERMAL SUPERMODELS PROJECT: AN UPDATE ON FLOW SIMULATOR DEVELOPMENT (Croucher)	40: DISTINGUISHING LIGHTER SHADES OF GREY: THE USE OF PORTABLE XRF TO DEFINE CHEMOSTRATIGRAPHY IN THE GREYWACKE BASEMENT OF NEW ZEALAND GEOTHERMAL SYSTEMS (White)	41: WATER QUALITY AND BIODIVERSITY SURVEY OF THREE WAIOTAPU GEOTHERMAL LAKES (Luketina)	54: SOCIETAL ACCEPTANCE OF REMOTE SENSING INNOVATIONS WITH AN EXAMPLE FROM WHAKAREWAREWA (Rae)
11:20	87: EXPERIMENTS WITH WAIWERA, A NEW GEOTHERMAL SIMULATOR (O'Sullivan)	48: 3D GEOLOGICAL MODELLING: AN ADVANCED METHODE TO BUILD GEOLOGICAL BASELINE MODEL IN HULULAIS GEOTHERMAL PROJECT, BENGKULU, INDONESIA (Nusantara)	102: RENEWABLE ENERGY OR RISKY TECHNOLOGY? – FRAMINGS OF DEEP GEOTHERMAL ENERGY IN GERMANY (Benighaus)	90: CASE STUDY: GROUND SOURCE THERMAL PILES (Sanderson)
11:40	21: RECENT ADVANCES IN THE COMPUTER MODELLING OF THE OHAAKI GEOTHERMAL SYSTEM (Batouis)	97: A 3D MODEL OF THE YAMAKAWA GEOTHERMAL SYSTEM: INSIGHTS INTO RESERVOIR STRUCTURE AND FUTURE FIELD MANAGEMENT (Widiatmojo)		113: THERMAL ROCK PROPERTIES – COMPARISONS OF APPARENT VALUES DETERMINED FROM IN-SITU TEMPERATURE PROFILES, AND VALUES DETERMINED BY LABORATORY MEASUREMENTS. (Seward)
12:00	**Lunch and Poster Session:** 8: THERMAL ACTIVITY EXPLORATION AND MONITORING OF RECENTLY ACTIVE KIRISHIMA VOLCANO IN THE SOUTHERN KYUSHU ISLAND IN JAPAN USING SATELLITE IMAGERIES (Mia) 19: GEOTHERMAL PROSPECTIVITY OF LOW-TEMPERATURE REGIONS IN NEW ZEALAND (Reyes) 49: UNDERSTANDING GEOTHERMAL RESERVOIRS USING 3D MODELLING TECHNIQUES: A CASE STUDY OF THE EMMO PROJECT, SOUTHERN JAPAN (O'Keeffe) 60: ON THE SUPERCRITICAL FLUID UNDER THE BRITTLE-DUCTILE BOUNDARY (Ogawa) 61: ORGANIZATION OF RESISTIVITY EXPLORATION DATA FOR DEVELOPMENT DEEP GEOTHERMAL SYSTEMS –REPROCESSING THE MAGNETOTELLURIC DATA AT KAKKONDA GEOTHERMAL FIELD, NE JAPAN (Tamaya) 84: PROBABILISTIC ASSESSMENT OF ELECTRICAL POTENTIAL OF TOCOMAR GEOTHERMAL FIELD (CENTRAL PUNA - NW ARGENTINA), USING VOLUMETRIC METHOD. (Barrios)			
13:00	Keynote 2 – Gudmundur Fridleifsson IDDP-2 – DRILLING INTO THE SUPERCRITICAL AT REYKJANES Room: Mokoia Room			

	Session 2.1: Modelling Room: Mokoia Room	**Session 2.2: Scaling** Room: Millennium 3	**Session 2.3: Geochemistry** Room: Millennium 1	**Session 2.4: Drilling** Room: Millennium 2
13:40	12: FORWARD AND INVERSE MODELLING OF GEOTHERMAL MICROSEISMICITY USING TOUGH2 COUPLED WITH AN EARTHQUAKE SIMULATOR (Rivera)	51: NANOSTRUCTURED CALCIUM SILICATE – A POTENTIAL SOLUTION TO PROBLEMATIC SILICA DEPOSITION FROM GEOTHERMAL BRINE AND A USEFUL PRODUCT (Johnston)	1: INVESTIGATING THE GEOTHERMAL SIGNATURE OF THE KAIMAI TUNNEL, NEW ZEALAND (Luketina)	100: KARKAR, ARMENIA – SLIMHOLE DRILLING AND TESTING RESULTS AND REMOTE PROJECT MANAGEMENT OVERVIEW (Austin)
14:00	37: NONLINEAR UNCERTAINTY QUANTIFICATION WITH A GEOTHERMAL MODEL (O'Sullivan)	9: RECOVERY OF NANO-STRUCTURED CALCIUM SILICATE HYDRATE FROM GEOTHERMAL BRINE USING A LAMELLA SEPARATOR (Borrmann)	13: X-RAY CHARACTERISATIONS OF SILICEOUS SINTER FROM STEAMBOAT SPRINGS GEOTHERMAL FIELD, NEVADA, USA (Qasim)	126: ADVANCED DYNAMICS FEA MODELING AS A NEW APPROACH TO IMPROVE GEOTHERMAL DRILLING PERFORMANCES IN INDONESIA (Mardiana)
14:20	64: INVESTIGATION OF PARAMETER UNCERTAINTY IN IDEALIZED GEOTHERMAL MODEL USING LINEAR UNCERTAINTY ANALYSIS (Omagbon)	10: A MODEL OF SILICA COLLOID GROWTH, STABILITY AND TRANSPORT USED TO PREDICT GEOTHERMAL REINJECTION LIFETIME (Chen)	14: APPLICATIONS OF SULFUR ISOTOPES IN CHARACTERIZING RESERVOIR PROCESSES AT THE KAWERAU GEOTHERMAL FIELD, NEW ZEALAND (Buscarlet)	125: DRILLING OPTIMIZATION IN HARD AND ABRASIVE GEOTHERMAL VOLCANIC ROCK USING THE INNOVATIVE CONICAL DIAMOND ELEMENT BIT (Mardiana)
14:40	35: A STUDY ON TETRAHEDRAL FINITE ELEMENTS (Pogacnik)	123: SCALING MITIGATIONS FOR THE GEOTHERMAL BINARY PLANT VAPORIZER: LEYTE, THE PHILIPPINES (Dariwsz)	53: EXPERIMENTAL DETERMINATION OF RATE CONSTANTS FOR THE BREAKDOWN OF THE ORGANIC TRACERS 1,3-NDS AND 2-NSA UNDER GEOTHERMAL CONDITIONS (Sajkowski)	118: ACID SOLUBILITY TESTING OF GREYWACKE CORE AND IMPLICATIONS FOR WELL PERMEABILITY ENHANCEMENT (Siratovich)
15:00	26: INTEGER PROGRAMMING OPTIMIZATION OF PRODUCTION WELL PLACEMENT (Adiga)	63: SILICA SCALE CONTROL IN NICARAGUA POWER PLANT (Delgado)		149: METHYLENE BLUE ANALYSIS OF CLAY SAMPLES FROM THE TIWI GEOTHERMAL FIELD (Gulacte)
15:20	Afternoon Tea			
	Session 3.1: Modelling Room: Mokoia Room	**Session 3.2 Scaling** Room: Millennium 3	**Session 3.3: Geochemistry** Room: Millennium 1	**Session 3.4: TVZ** Room: Millennium 2
15:40	79: NUMERICAL MODELLING OF THE INFLUENCE OF GEOLOGY AND GROUNDWATER RECHARGE ON GEOTHERMAL ACTIVITY IN THE CENTRAL TVZ (Pearson-Grant)	131: CHEMICAL CLEANING AND REJUVENATION OF GEOTHERMAL WELLS AND SURFACE EQUIPMENT (Gill)	37: BASALT-SEAWATER INTERACTION AT NEAR SUPERCRITICAL CONDITIONS: HYDROTHERMAL ALTERATION IN THE SUB-SEAFLOOR (Fabbrizio)	67: THE DEEP CONTROL(S) OF HIGH ENTHALPY GEOTHERMAL SYSTEMS: A MULTIDISCIPLINARY PERSPECTIVE (Chambefort)
16:00	83: GENERATION OF ALTERNATIVE GEOLOGICAL MODELS FOR SPATIAL UNCERTAINTY IN A GEOTHERMAL CONTEXT (Vidal)	58: H2S CORROSION OF CARBON STEEL IN GEOTHERMAL FLUIDS (Ghazi)	47: A NUMERICAL METHOD FOR PREDICTING THERMOPHYSICAL PROPERTIES OF COMPLEX CHLORIDE-DOMINATED BRINES (Walsh)	105: GROUNDWATER CIRCULATION SYSTEMS OF HIGH-TEMPERATURE GEOTHERMAL FIELDS IN THE UPPER WAIKATO CATCHMENT, TAUPO VOLCANIC ZONE, NEW ZEALAND (White)
16:20	124: 3D NATURAL STATE MODEL OF KARAHA-TALAGA BODAS GEOTHERMAL FIELD, WEST JAVA, INDONESIA (Prasetyo)	65: THE MATERIAL CORROSION TEST USING LOOP SYSTEM UNDER ACIDIC CONDITION AT GEOTHERMAL FIELD IN JAPAN (Yanagisawa)	85: FINGERPRINTING THE TEMPERATURE AND FLUID SOURCE OF CALCITE IN GEOTHERMAL SYSTEMS USING CLUMPED ISOTOPES (Mölich)	25: TECTONIC STRUCTURE AND PERMEABILITY IN THE TAUPO RIFT: NEW INSIGHTS FROM ANALYSIS OF LIDAR DERIVED DEMS (Villamor)
16:40	116: THE SUBSURFACE GEOMETRY OF A NATURAL GEOTHERMAL RESERVOIR (Wallis)	32: DEVELOPMENT OF NEW FIELD TESTING TOOLS FOR GEOTHERMAL POWER PLANT RISK ASSESSMENT OF CORROSION AND SCALING (Osato)	88: PROGRESSIVE DEVOLATISATION OF NEW ZEALAND RESERVOIR ROCKS FROM SUB-CRITICAL TO SUPERCRITICAL CONDITIONS (Mountain)	
17:00	23: GEOMETRICAL MODELLING OF FRACTURE NETWORKS IN AN ANDESITE-HOSTED GEOTHERMAL RESERVOIR. (Kissling)	122: ANALYSIS ON SCALING PROBLEM IN INJECTION FACILITIES: A CASE FROM MUARA LABUH GEOTHERMAL FIELD, INDONESIA (Alfeddy)	106: ASSESSMENT OF CHEMICAL ANTISCALANT IN CONTROLLING SILICA SCALING AT WAIRAKEI BINARY PLANT, NEW ZEALAND (SEASTRES)	
17:20 19:00	Welcome Reception including WING speakers			

NZGW 2017 Programme

Thursday 23 November 2017

8:30	NZGA AGM Room: Makaia Room		
9:00	Housekeeping Room: Makaia Room		
9:10	Keynote 3 - James Faulds DISCOVERING NEW GEOTHERMAL SYSTEMS IN THE GREAT BASIN REGION, WESTERN USA: AN INTEGRATED APPROACH FOR ESTABLISHING GEOTHERMAL PLAY FAIRWAYS Room: Makaia Room		
10:00	Morning Tea		
	Session 4.1: Production Room: Makaia Room	Session 4.2: Geophysics Room: Millenium 3	Session 4.3: Other Room: Millenium 1
10:20	27: THE GEOTHERMAL TWO-PHASE ORIFICE PLATE (Mubarek)	99: A STUDY OF PARAMETER COUPLING IN MT AND GRAVITY JOINT INVERSION FOR GEOTHERMAL EXPLORATION (Tartis)	7: THE UTAH FRONTIER OBSERVATORY FOR GEOTHERMAL RESEARCH (FORGE): A LABORATORY FOR EGS DEVELOPMENT (Moore)
10:40	44: COUPLED GEOTHERMAL PROCESS AND RESERVOIR MANAGEMENT (Dabbour)	58: ON THE AIRBORNE SURVEY BY A HELICOPTER- A BRIEF OUTLINE AND SEVERAL ANALYSES OF THE SURVEY (Tosha)	69: ANALYSIS OF NEW INDONESIAN GEOTHERMAL BPP-TARIFF AND IMPACT OF FEASIBILITY OF GEOTHERMAL PLANTS IN EASTERN INDONESIA IN THE NEXT DECADE (Van Campen)
11:00	50: THE APPLICATION OF HELICAL SCREW EXPANDING TECHNOLOGY FOR GEOTHERMAL POWER GENERATION (Hooper)	62: INTEGRATED ANALYSIS USING 3D SEISMIC SURVEY IN THE YAMAGAWA GEOTHERMAL FIELD, SOUTHWESTERN JAPAN (Mouri)	116: REASSESSMENT OF ITB RESEARCH CONTRIBUTION TO POWER PLANT PERFORMANCE IMPROVEMENT (Sanjamahoo)
11:20	76: HYDROGEN PEROXIDE AS A GEOTHERMAL COOLING WATER BIOCIDE (Clark)	94: GEOTHERMAL TEMPERATURE ESTIMATION BASED ON RESISTIVITY DATA USING ARTIFICIAL NEURAL NETWORK: APPLICATION TO THE KAKKONDA GEOTHERMAL FIELD, JAPAN (Ishisuka)	81: REVIEW ON OHAAKI CONSENTING, MODELLING AND RESOURCE ASSESSMENT: THE BEST PLACE TO LOOK FOR LESSONS ON SUSTAINABLE GEOTHERMAL OPERATION AND MONITORING (Van Campen)
11:40	18: WELLBORE MODELING IN DRY STEAM PRODUCTION WELL IN GEOTHERMAL MULTI LATERAL WELL (Guwewijoyo)	24: PRELIMINARY INVESTIGATION OF SEISMIC VELOCITY VARIATION AT THE ROTOKAWA AND NGATAMARIKI GEOTHERMAL FIELDS (Sewell)	29: REASSESSMENT OF GEOTHERMAL ENERGY POTENTIAL IN TATAPANI GEOTHERMAL FIELD IN BALRAMPUR DISTRICT, CHHATTISGARH STATE, INDIA (Patbhaje)
12:00	Lunch		
13:00	Keynote 4 - Initiating Māori Engagement - included in Oil & Kaitiakitanga Future Geothermal Innovation and Office Use Tapaeruki Nicholson, president of Te Waiariki, Māori Geothermal Advisory Group, Te Pūmautanga o Te Arawa Trust Room: Makaia Room		
	Session 5.1: Production Room: Makaia Room	Session 5.2: Geophysics Room: Millenium 3	Session 5.3: Direct Use Room: Millenium 1
13:40	130: GEOTHERMAL STEAM WATER SEPARATOR SIZING FOR OPTIMIZING INVESTMENT IN POWER DEVELOPMENT (Zarrouk)	125: QUANTITATIVE ANALYSIS OF EARTHQUAKE ENERGY INDUCED BY WATER INJECTION (Ishikawa)	38: GEOTHERMAL ECONOMIC DEVELOPMENT IN NEW ZEALAND - USING A "KISSING FROGS" APPROACH (Blair)
14:00	71: TESTING OF CYCLONE SEPARATORS AND STEAM PIPELINES FOR SEPARATION AND SCRUBBING PERFORMANCE (Mise)	128: IDENTIFYING FAULTS AND FRACTURES AT DIFFERENT DEPTHS FROM AIRBORNE GRAVITY GRADIENT SURVEYS OVER KUJYU AND KIRISHIMA GEOTHERMAL AREAS, JAPAN (Soengsene)	2: OPPORTUNITIES FOR INDUSTRIAL CO-LOCATION TO IMPROVE RENEWABLE ENERGY USE AND EFFICIENCY (Alcaraz)
14:20	117: STEAM PURITY CHALLENGES IN GEOTHERMAL POWER PLANTS: A CASE OF OLKARIA IAU POWER PLANT (Wafula)	129: APPLYING INNOVATIONS IN MT TECHNOLOGY FOR REDUCING GEOTHERMAL EXPLORATION RISKS (Daud)	43: BUILDING A SUSTAINABLE CITY UTILISING GEOTHERMAL HEAT PUMPS – THE CHRISTCHURCH STORY. (Seward)
14:40	89: TE MIHI GEOTHERMAL POWER STATION - FAR FIELD NOISE MITIGATION TO THE TE MIHI COOLING TOWERS (Morrison)	22. A DISCUSSION BETWEEN A RESERVOIR ENGINEER AND A GEOLOGIST: INTEGRATING BOREHOLE IMAGE LOGS AND COMPLETION TEST DATA (Massie)	
15:00	90: TE MIHI GEOTHERMAL POWER STATION - HOTWELL PUMPS – A TALE OF UNINTENDED CONSEQUENCES (Morrison)	33: A NATURAL STATE MODELLING OF ULUMBU GEOTHERMAL FIELD, EAST NUSA TENGGARA, INDONESIA (Kurniawan)	
15:20	Afternoon Tea		

	Session 6.1: Room: Makaia Room
15:45	Japan - industry updates
16:15	Indonesia Geothermal Centre of Excellence
16:45	ESG - ways in which Oil & Gas can work with Geothermal
17:00	Industry Panel
18:30	Travel to Dinner venue
19:00	NZGW Dinner
22:30	Blue Baths, Queens Drive, Experiment Gardens

Friday 24 November 2017

	Room: Makaia Room
9:00	Housekeeping & NZGA Welcome
9:20	MBIE
9:30	MFAT
9:40	NZTE
9:50	NZTE
10:00	NZTE
10:10	AGF
10:20	GeoNZ
10:30	Morning Tea
11:00	Geothermal Institute
11:10	Jacobs
11:20	Seequent
11:30	Mill Century
11:40	BOPRC
11:50	Contact
12:00	Nalco
12:30	Lunch

Friday 24 November 2017

	Room: Millenium Room
13:30	WINZ
13:40	GNS Science
13:50	Tauhara North No 2
14:00	HERA
14:10	WRC
14:20	Mercury
14:30	MTL
14:40	Top Energy
14:50	Utrex
15:00	Afternoon Tea
15:30	Thornton Cook
15:40	AECOM
15:50	
16:00	
Awards	NZGA Innovation Award
	Awards for best papers
17:00	Workshop Closes

39th NZGW New Zealand Geothermal Workshop

DFDP-2 GEOTHERMAL DISCOVERY IN WESTLAND, NEW ZEALAND

Rupert Sutherland[1], John Townend[1], Virginia Toy[2]

[1]Victoria University of Wellington, PO Box 600, Wellington, New Zealand

[2] University of Otago, PO Box 56, Dunedin, New Zealand

rupert.sutherland@vuw.ac.nz

Keywords: *earthquake, tectonics, geothermal, Alpine Fault, hydrogeology.*

ABSTRACT

Boreholes drilled as part of the Deep Fault Drilling Project (DFDP) reveal a geothermal system in the hanging-wall of the Alpine Fault. The DFDP-2B discovery of 100°C water at 600 m depth beneath farmland adjacent to State Highway 6 near Whataroa has led to local interest in geothermal energy, and whether other Westland valleys also have resource potential. The hot temperatures are caused by a combination of fault slip, which moves rock and heat from depth, and topographically-driven fluid flow through fractured rocks that concentrates heat into valleys. Additional technical work is required to assess the size, quality and safety of the geothermal system, but the discovery provides an exciting opportunity for regional development based on clean sustainable energy that can directly leverage existing plant and people employed in a mining industry that is in long-term decline.

1. INTRODUCTION

The Deep Fault Drilling Project (DFDP) is a multi-stage scientific investigation of the Alpine Fault in western South Island, New Zealand (Townend et al., 2009). The first stage of the project (DFDP-1) drilled to 152 m depth at Gaunt Creek (Cooper and Norris, 1994) and was completed in 2011 (Boulton et al., 2014; Carpenter et al., 2014; Niemeijer et al., 2016; Schleicher et al., 2015; Sutherland et al., 2011; Sutherland et al., 2012; Townend et al., 2013; Toy et al., 2015). The second stage of the project (DFDP-2) was completed nearby in the Whataroa valley (Fig. 1) in January 2015 and reached a drilled depth of 893 m (Sutherland et al., 2015).

The science questions that DFDP originally aimed to address are related to fault zone processes. How and why do earthquakes happen? How does slip on a large geological fault occur? What are the ambient conditions and physical properties on and around an active fault in its pre-earthquake state?

The DFDP-2B borehole did not achieve all of its technical objectives, due to a casing failure during a cementing operation, but yielded a remarkable discovery. The geothermal gradient was much higher than expected and comparable to geothermal boreholes that have been drilled in the Taupo Volcanic Zone (Sutherland et al., 2017). There is no evidence for Neogene volcanic activity anywhere near the DFDP-2 site. This paper presents a summary of what was discovered, an explanation for the extreme hydrothermal conditions, and discussion of potential implications for geothermal energy resources in the western South Island.

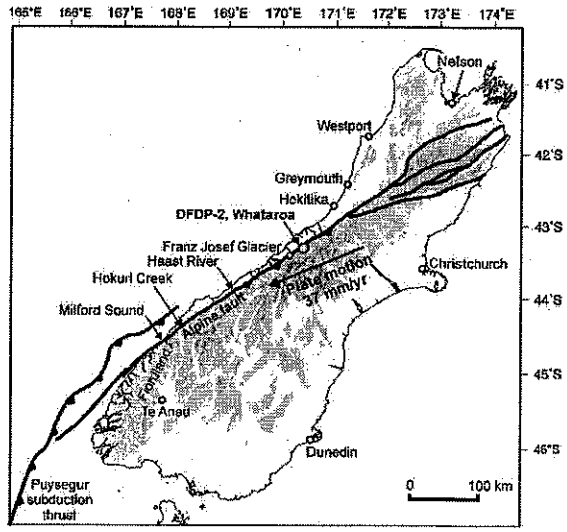

Figure 1: Location of the DFDP-2 site at Whataroa. DFDP-1 was completed at Gaunt Creek, 7 km southwest of DFDP-2.

2. THE ALPINE FAULT

The Alpine Fault (Fig. 1) is a mature plate-bounding transpressive structure that has accommodated >460 km of dextral offset since 24 Ma (Sutherland, 1999), and has a late Quaternary average slip rate of 27+/-5 mm/yr (Norris and Cooper, 2001). The hanging-wall is Mesozoic amphibolite facies meta-greywacke that has been deformed into protomylonite, mylonite, and cataclasite with increasing proximity to the principal slip zone (Norris and Cooper, 2007). The foot-wall is composed of Paleozoic granitoids that intrude quartzose metasediments.

The Alpine Fault fails in large earthquakes (MW 7.6–8.2) every 200–400 years and last ruptured in AD 1717, so is close to rupturing again (Sutherland et al., 2007). Oblique-reverse motion has exhumed a suite of fault rocks from depths of 30 km over the past 3-5 million years (Norris and Cooper, 2007). Numerical models indicate that rapid rock exhumation advects isotherms to relatively shallow depths, and this has been used to explain the occurrence of many hot (<58°C) springs in the hanging-wall of the central Alpine Fault (Allis and Shi, 1995; Allis, 1981; Koons, 1987).

3. DFDP RESULTS

The DFDP-1A and DFDP-1B boreholes penetrated fractured protomylonite, cataclasite, fault gouge, and Quaternary sediments (Sutherland et al., 2011; Sutherland et al., 2012; Toy et al., 2015). The principal slip zone fault gouge is a through-going, planar, thin (1-50 cm, mostly <10 cm) layer of extremely fine-grained

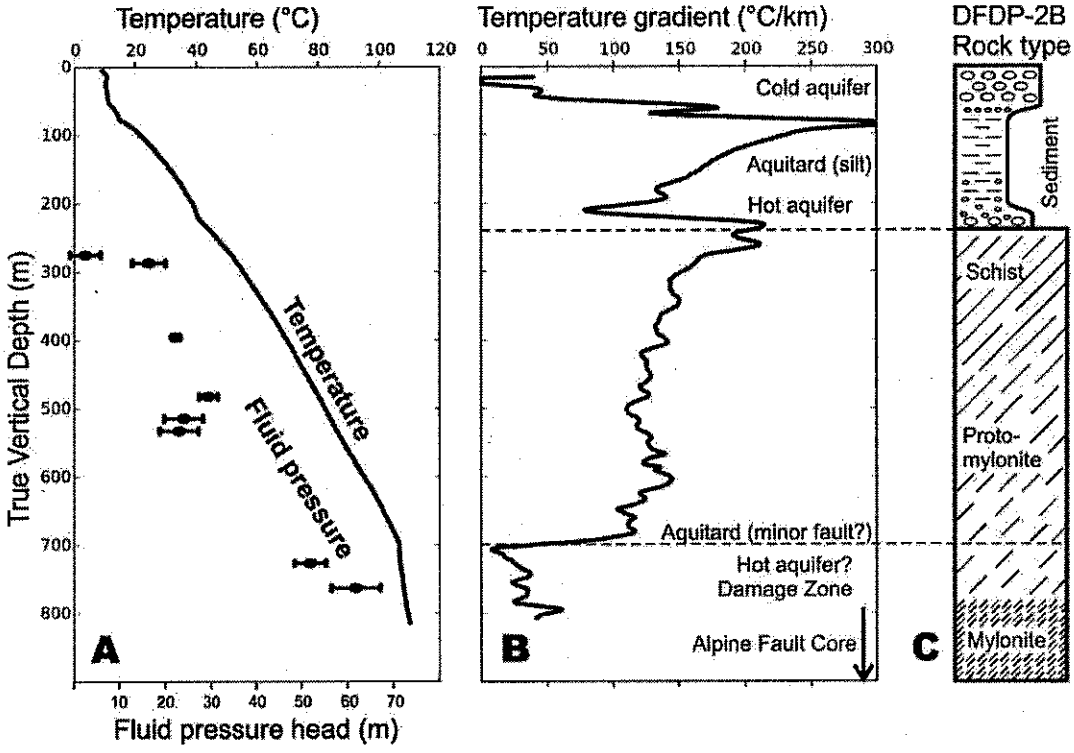

Figure 2. DFDP-2B drilling results. Fluid pressure observations made during breaks in drilling (A). Long-term post-drilling temperature profile measured using distributed temperature sensing on a fibre optic cable (A). Temperature gradient (B). Simplified geologic log and interpretation (C). After Sutherland et al. (2017)

rock generated by slip during repeated earthquakes. The gouge and cemented cataclasite represent a continuous and impermeable layer of variable thickness that plays a major role in governing how fluids move within the fault zone (Sutherland et al., 2012). The DFDP-1B borehole (152 m depth) has a geothermal gradient of 62.6 ± 2.1 °C/km. Wireline geophysical logs reveal a complex pattern of fracturing and alteration that is asymmetric across the fault zone (Townend et al., 2013).

Hydraulic observations and laboratory experiments reveal that cataclasite and the principal-slip-zone gouge (which probably forms a near-continuous layer for hundreds of km along strike and extends to a few km depth) have permeability $<10^{-19}$ m^2 and form an aquitard, whereas fractured protomylonite that is found in the fault hanging-wall (i.e. a continuous tabular zone overlying and parallel to the low-permeability gouge layer) has much higher permeability of $>10^{-15}$ m^2 (Boulton et al., 2012; Sutherland et al., 2012).

The DFDP-2B borehole penetrated a sequence of Quaternary gravel and lake silt, schist, protomylonite, and mylonite (Fig. 2) (Sutherland et al., 2017; Toy et al., 2017). The base of the borehole is estimated to be within 200–400 m of the principal slip zone (PSZ) gouge, based on site surveys and measurement of quartz grain sizes and microstructures in drill cuttings that are similar to mylonitic fault rocks exposed nearby. Comprehensive rock, mud, wireline, and seismological observations were collected, and a fibre-optic cable was installed after drilling to acquire repeated precise temperature measurements.

Post-drilling equilibrated temperatures in the borehole reveal a zone above 700 m depth (true vertical; 740 m drilled depth) characterized by a thermal gradient of 100–200°C/km, and a deeper zone with a gradient of 30–50°C/km (Fig. 2). The fluid pressure gradient in the borehole below the sedimentary layers is 8–10% above hydrostatic, but an aquifer at the base of the sediments (230–240 m) is only slightly over-pressured (<5 m head). This means that, unlike the PSZ gouge mentioned above, the Quaternary silts do not form an effective hydraulic seal (Fig. 2).

The geothermal gradient in the upper 700 m of the DFDP-2B borehole is unusual by global standards: 99% of geothermal gradients measured in deep (>500 m) boreholes elsewhere are <80°C/km (Pollack et al., 1993). Values exceeding 80°C/km are typically associated with volcanic regions, such as the Taupo Volcanic Zone, but there is no evidence for Neogene volcanism near the DFDP-2B site. The regional value determined from petroleum boreholes west of DFDP-2B is c. 30°C/km (Townend, 1999).

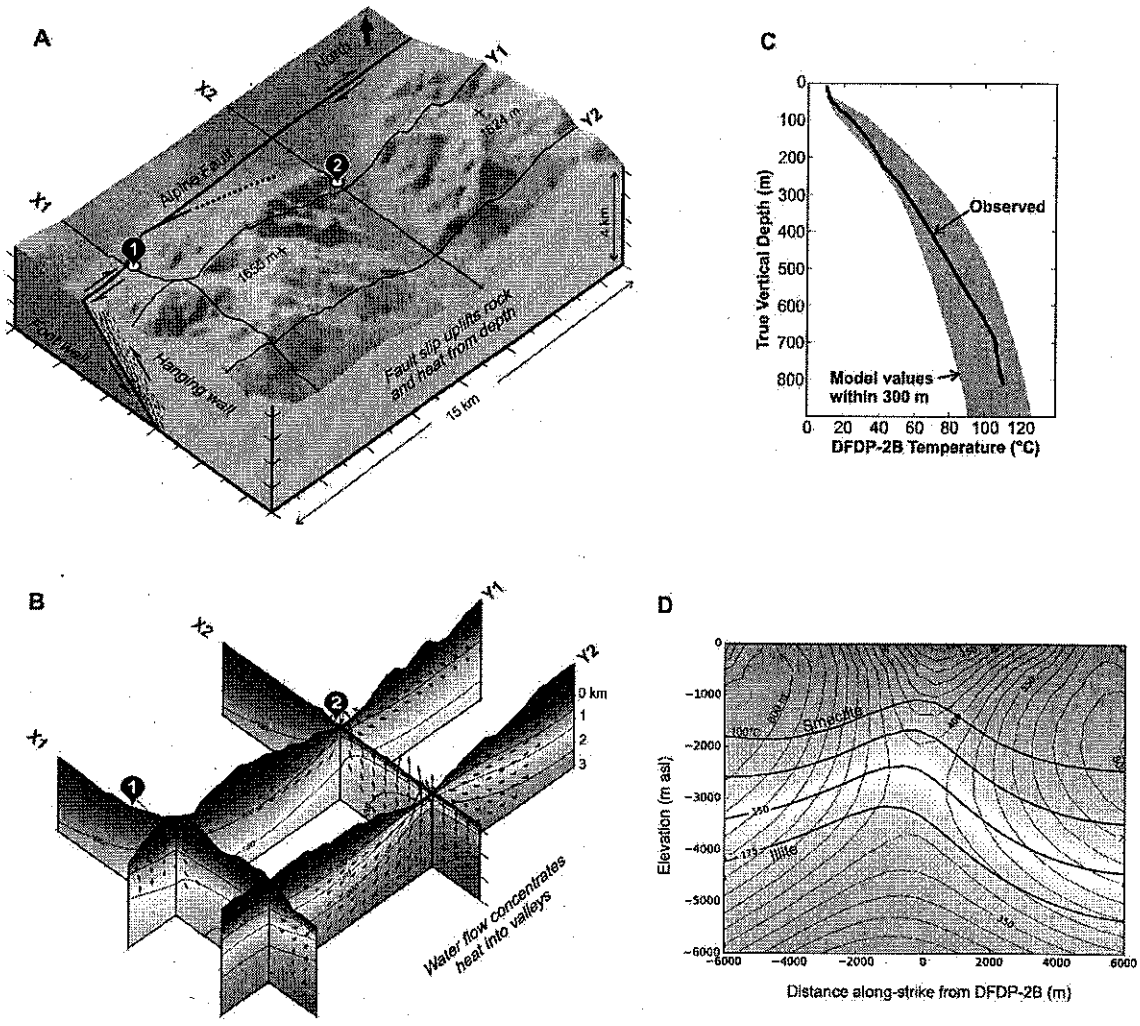

Figure 3. Thermal and fluid flow models, after Sutherland et al. (2017). (A) DFDP-1 and DFDP-2 locations (marked 1 and 2, respectively). (B) Temperature cross-sections with contours in °C and fluid fluxes (arrows show fluxes >0.15 m/yr) extracted from a 3D numerical model with 200 m horizontal resolution near DFDP-2. Parameters for model shown are: (1) dip-slip rate of 8 mm/yr; and (2) uniform permeability of 5.0×10^{-16} m^2 in a layer above 5 km bsl within the Alpine Fault hanging-wall. (C) Comparison of model values (as shown in B), extracted from within 300 m of DFDP-2B, with borehole observations. (D) Fluid pressure and temperature inferred on the Alpine Fault plane: thin lines are fluid pressure head (m, reference fluid density at surface); and bold lines are temperature contours approximately equivalent to the temperature of illite-smectite transitions (100–175°C).

4. GEOTHERMAL STATE

Sutherland et al. (2017) modelled the thermal state near DFDP sites by considering heat transport via:
(1) conduction;
(2) rock advection driven by fault slip; and
(3) fluid advection driven by local topography (Fig. 3).
We assumed uniform high permeability to some fixed depth (3 or 5 km) above the principal slip zone of the Alpine Fault and low permeability beneath it. Adjustable parameters were the maximum value of permeability, and the rate of reverse dip-slip fault movement, which is constrained by geological observations of late Quaternary offsets to lie within the range 6–14 mm/yr near the drill-site (Norris and Cooper, 2007). Drilling-related temperature anomalies were modelled separately and excluded from our analysis by selecting observations made >6 months after drilling. There is little variability in thermal diffusivity within the borehole. The 3D model domain is much larger than the specific region of interest.

We aimed to fit temperature observations from DFDP-2B (Fig. 2) and the geothermal gradient of 62±2°C/km measured in the 150 m-deep DFDP-1B borehole (Fig. 3) (Sutherland et al., 2012). Our models are intentionally simplified, because they are under-constrained by observations, and intended only to gain general insight into hydrothermal structure in and around the fault zone. The best fit to DFDP-2B temperature observations is obtained with a fault dip-slip rate of 14 mm/yr and low permeability, but this solution does not fit DFDP-1B observations. The relatively low average curvature of the thermal profile, combined with the over-simplified hydrological structure, leads to the conclusion

that rock advection and thermal diffusion are the primary heat transport mechanisms at 240–740 m depth in DFDP-2B. However, but the large difference in geothermal gradient between DFDP-1B and DFDP-2B requires that fluid advection plays an important heat transfer role between sites and requires a regional value of permeability $>5\times10^{-16}$ m^2. The DFDP-2B fluid pressure gradient indicates upward flow through the fractured rock mass near the borehole (Fig. 2A). The large difference in geothermal gradient between sites is explained by along-strike variations in topography that drive fluid flow and hence advection of heat (Fig. 3).

The model results are broadly consistent with existing knowledge of fault slip rate and heterogeneous rock permeability in the hanging-wall of the Alpine Fault. We expect permeability to be low within cataclasites near the principal slip zone and minor fault splays (Sutherland et al., 2012), and for them to be barriers to fault-normal flow. We expect high permeability within the damage zone, producing an aquifer that enhances fault-parallel flow, and beneath mountains of the hanging wall where warm springs are common (Cox et al., 2015). The region of relatively-low geothermal gradient at the base of DFDP-2B (Fig. 2) is a discrete hydrological domain and interpreted as an aquifer associated with the damage zone, but we were unable to verify its properties due to engineering difficulties. Fluid pressure equilibration experiments ("slug tests") conducted during drilling of DFDP-2B indicate bulk-rock permeability around the borehole of order 10^{-15} m^2. However, these estimated values are significantly affected (reduced) by the bentonite mud system that was used during drilling.

In summary, we infer that fault slip moves rock and heat from depth, and topographically-driven fluid flow through fractured rocks concentrates heat into valleys (Fig. 3).

5. ECONOMIC POTENTIAL

The discovery of 100°C water at 600 m depth beneath farmland adjacent to State Highway 6 near Whataroa has led to a great deal of local interest into whether geothermal energy could be commercialized, and whether other Westland valleys may also contain geothermal resources. There are natural warm springs in most valleys.

Commercial success will depend on several factors:
(1) size and sustainability of the resource, i.e. how much heat can be extracted;
(2) quality of the resource, i.e. how rapidly that heat can be extracted;
(3) value of the commercial end-use; and
(4) if the extraction of hot water can be done safely with minimal environmental risk, i.e. regulation and social license.

Additional drilling is required to assess the spatial and depth extent of the geothermal system. However, the very large number of wireline logging runs that we carried out during the DFDP-2 experiment may already allow us to estimate hydraulic conductivities of individual fractured zones, and hence we may be able to construct preliminary reservoir models and estimate the rate at which fluid could be produced. This is a work in progress that we would value input into.

The value of commercial end use is hard to assess without better information regarding characteristics of the resource (size, quality, safety). Models predict that maximum temperatures available may be about 180-240°C. The region is remote and would benefit from local electricity supply for domestic use, tourism, and agriculture; but the total size of demand is relatively small. Resilience may be improved by local supply, if infrastructure is built to withstand earthquake effects. It is likely that earthquakes would enhance permeability and hence increase fluid production rates and 'quality' of the resource. It may be that the direct use of heat, e.g. for milk processing, tourism, and agriculture, could provide greater value than electricity production. Further work is required to assess the value proposition of the resource.

The safety of geothermal production is a significant concern, because the system is bound by the Alpine Fault, which is one of the most hazardous faults in New Zealand. Geothermal production is known to induce earthquakes in some locations. We are in a good position to monitor and model this process at DFDP-2, with good instrumentation in place, a catalogue of background earthquake activity (Chamberlain et al., 2017), and a large research team that specializes in earthquake science. The chemistry of deep geothermal fluids is unknown at present, but is likely to be predictable and relatively benign, based on existing knowledge of hot spring chemistry (Menzies et al., 2014).

The size and quality of the total Westland resource remains highly uncertain. It was previously known that many valleys have minor hot springs with typical temperatures of 20-40°C, and the low temperatures and flow rates provided little encouragement for geothermal exploration. Our discovery reveals that temperatures beneath major valleys may be much higher at moderate depths than previously thought; but that this heat is masked by thick gravel aquifers with active cold groundwater systems.

Additional technical work is required to assess the size, quality and safety of the geothermal system, but the discovery opens up an exciting opportunity for regional development based on clean sustainable energy. Of particular appeal is that the engineering required to develop this resource can directly leverage off existing plant and people that are employed in a local mining industry that is in long-term decline. It is surely worth further investigation.

ACKNOWLEDGEMENTS

This paper is based heavily on the publication of Sutherland et al. (2017) and work of the broader DFDP-2 Science Team, particularly the hydrological models produced by Phaedra Upton and Jamie Coussens. We thank: the Friend family for land access and the Westland community for support; Schlumberger for assistance with optical fibre technology; Benson, Conze, Marx, Pooley, Pyne, and Yeo for engineering and site support; the CNRS University of Montpellier wireline logging group of Pezard, Henry, Nitsch, and Paris; Arnold Contracting; Eco Drilling; and Webster Drilling. Funding was

provided by the International Continental Scientific Drilling Program (ICDP), NZ Marsden Fund, GNS Science, Victoria University of Wellington, University of Otago, NZ Ministry for Business Innovation and Employment, NERC grants NE/J022128/1 and NE/J024449/1, and Netherlands Organization for Scientific Research VIDI grant 854.12.011 and ERC starting grant SEISMIC 335915. ICDP provided expert review, staff training, and technical guidance.

REFERENCES

Allis, R., and Shi, Y., 1995, New insights to temperature and pressure beneath the central Southern Alps, New Zealand: New Zealand Journal of Geology and Geophysics, v. 38, no. 4, p. 585-592.

Allis, R. G., 1981, Continental underthrusting beneath the Southern Alps of New Zealand: Geology, v. 9, p. 303-307.

Boulton, C., Carpenter, B. M., Toy, V., and Marone, C., 2012, Physical properties of surface outcrop cataclastic fault rocks, Alpine Fault, New Zealand: Geochemistry Geophysics Geosystems v. Q01018, p. doi:10.1029/2011GC003872.

Boulton, C., Moore, D. E., Lockner, D. A., Toy, V. G., Townend, J., and Sutherland, R., 2014, Frictional properties of exhumed fault gouges in DFDP-1 cores, Alpine Fault, New Zealand: Geophysical Research Letters, v. 41, no. 2, p. 356-362.

Carpenter, B., Kitajima, H., Sutherland, R., Townend, J., Toy, V., and Saffer, D., 2014, Hydraulic and acoustic properties of the active Alpine Fault, New Zealand: Laboratory measurements on DFDP-1 drill core: Earth and Planetary Science Letters, v. 390, p. 45-51.

Chamberlain, C. J., Boese, C. M., Eccles, J. D., Savage, M. K., Baratin, L. M., Townend, J., Gulley, A. K., Jacobs, K. M., Benson, A., Taylor-Offord, S., Thurber, C., Guo, B., Okada, T., Takagi, R., Yoshida, K., Sutherland, R., and Toy, V. G., 2017, Real-Time Earthquake Monitoring during the Second Phase of the Deep Fault Drilling Project, Alpine Fault, New Zealand: Seismological Research Letters, v. 88, p. 1443-1454.

Cooper, A. F., and Norris, R. J., 1994, Anatomy, structural evolution, and slip rate of a plate-boundary thrust: The Alpine fault at Gaunt Creek, Westland, New Zealand: Geological Society of America Bulletin, v. 106, p. 627-633.

Cox, S., Menzies, C., Sutherland, R., Denys, P., Chamberlain, C., and Teagle, D., 2015, Changes in hot spring temperature and hydrogeology of the Alpine Fault hanging wall, New Zealand, induced by distal South Island earthquakes: Geofluids, v. 15, no. 1-2, p. 216-239.

Koons, P. O., 1987, Some thermal and mechanical consequences of rapid uplift; an example from the Southern Alps, New Zealand: Earth and Planetary Science Letters, v. 86, no. 2, p. 307-319.

Menzies, C. D., Teagle, D. A., Craw, D., Cox, S. C., Boyce, A. J., Barrie, C. D., and Roberts, S., 2014, Incursion of meteoric waters into the ductile regime in an active orogen: Earth and Planetary Science Letters, v. 399, p. 1-13.

Niemeijer, A., Boulton, C., Toy, V., Townend, J., and Sutherland, R., 2016, Large-displacement, hydrothermal frictional properties of DFDP-1 fault rocks, Alpine Fault, New Zealand: Implications for deep rupture propagation: Journal of Geophysical Research: Solid Earth, v. 121, no. 2, p. 624-647.

Norris, R. J., and Cooper, A. F., 2001, Late Quaternary slip rates and slip partitioning on the Alpine Fault, New Zealand: Journal of Structural Geology, v. 23, no. 2-3, p. 507-520.

Norris, R. J., and Cooper, A. F., 2007, The Alpine Fault, New Zealand: surface geology and field relationships, *in* Okaya, D., Stern, T. A., and Davey, F., eds., A Continental Plate Boundary: Tectonics at South Island, New Zealand, American Geophysical Union, p. 157–175.

Pollack, H. N., Hurter, S. J., and Johnson, J. R., 1993, Heat flow from the Earth's interior: analysis of the global data set: Reviews of Geophysics, v. 31, no. 3, p. 267-280.

Schleicher, A., Sutherland, R., Townend, J., Toy, V., and van der Pluijm, B., 2015, Clay mineral formation and fabric development in the DFDP-1B borehole, central Alpine Fault, New Zealand: New Zealand Journal of Geology and Geophysics, v. 58, no. 1, p. 13-21.

Sutherland, R., 1999, Cenozoic bending of New Zealand basement terranes and Alpine Fault displacement: a brief review: New Zealand journal of geology and geophysics, v. 42, p. 295-301.

Sutherland, R., Eberhart-Phillips, D., Harris, R. A., Stern, T., Beavan, J., Ellis, S., Henrys, S., Cox, S., Norris, R. J., Berryman, K. R., Townend, J., Bannister, S., Pettinga, J., Leitner, B., Wallace, L., Little, T. A., Cooper, A. F., Yetton, M., and Stirling, M., 2007, Do great earthquakes occur on the Alpine fault in central South Island, New Zealand?, *in* Okaya, D., Stern, T. A., and Davey, F., eds., A Continental Plate Boundary: Tectonics at South Island, New Zealand, American Geophysical Union, p. 235–251.

Sutherland, R., Townend, J., Toy, V., Allen, M., Baratin, L., Barth, N., Beacroft., Benson, l., Boese, C., Boles, A., Boulton, C., Capova, l., Carpenter, B., Celerier, B., Chamberlain, C., Conze, R., Cooper, A., Coussens, J., Coutts, A., Cox, S., Craw, L., Doan, M., Eccles, J., Faulkner, D., Grieve, J., Grochowski, J., Gulley, A., Henry, G., Howarth, J., Jacobs, K., Jeppson, T., Kato, N., Keys, S., Kirilova, M., Kometani, Y., Kovacs, A., Langridge, R., Lin, W., Little, T., Mallyon, D., Mariani, B., Marx, R., Massiot, C., Mathewson, L., Melosh, B., Menzies, C., Moore, J., Morales, L., Morgan, C., Mori, H., Niemeijera, A., Nishikawa, O., Nitsch, O., Paris Cavailhès, J., Pooley, B., Prior, D., Pyne,

A., Sauer, K., Savage, M., Schleicher, A., Schmitt, D., Shigematsu, N., Taylor-Offord, S., Tobin, H., Upton, P., Valdez, R., Weaver, K., Wiersberg, T., Williams J., Yeo, S., and Zimmer, M., 2015, Deep Fault Drilling Project (DFDP), Alpine Fault boreholes DFDP-2A and DFDP-2B technical completion report: GNS Science Report, v. 2015/50, p. 1-269.

Sutherland, R., Townend, J., Toy, V., Upton, P., Coussens, J., Allen, M., Baratin, L. M., Barth, N., Becroft, L., Boese, C., Boles, A., Boulton, C., Broderick, N. G. R., Janku-Capova, L., Carpenter, B. M., Célérier, B., Chamberlain, C., Cooper, A., Coutts, A., Cox, S., Craw, L., Doan, M. L., Eccles, J., Faulkner, D., Grieve, J., Grochowski, J., Gulley, A., Hartog, A., Howarth, J., Jacobs, K., Jeppson, T., Kato, N., Keys, S., Kirilova, M., Kometani, Y., Langridge, R., Lin, W., Little, T., Lukacs, A., Mallyon, D., Mariani, E., Massiot, C., Mathewson, L., Melosh, B., Menzies, C., Moore, J., Morales, L., Morgan, C., Mori, H., Niemeijer, A., Nishikawa, O., Prior, D., Sauer, K., Savage, M., Schleicher, A., Schmitt, D. R., Shigematsu, N., Taylor-Offord, S., Teagle, D., Tobin, H., Valdez, R., Weaver, K., Wiersberg, T., Williams, J., Woodman, N., and Zimmer, M., 2017, Extreme hydrothermal conditions at an active plate-bounding fault: Nature, v. 546, no. 7656, p. 137-140.

Sutherland, R., Toy, V., Townend, J., Eccles, J., Prior, D. J., Norris, R. J., Mariani, E., Faulkner, D. R., DePascale, G., Carpenter, B. M., Boulton, C., Menzies, C. D., Cox, S., Little, T., Hasting, M., Cole-Baker, J., Langridge, R., Scott, H. R., Reid-Lindroos, Z. R., Fleming, B., and Wing, R., 2011, Operations and well completion report for boreholes DFDP-1A and DFDP-1B, Deep Fault Drilling Project, Alpine Fault, Gaunt Creek, New Zealand: GNS Science Report, v. 2011/48, p. 70.

Sutherland, R., Toy, V. G., Townend, J., Cox, S. C., Eccles, J. D., Faulkner, D. R., Prior, D. J., Norris, R. J., Mariani, E., Boulton, C., Carpenter, B. M., Menzies, C. D., Little, T. A., Hasting, M., De Pascale, G. P., Langridge, R. M., Scott, H. R., Lindroos, Z. R., Fleming, B., and Kopf, A. J., 2012, Drilling reveals fluid control on architecture and rupture of the Alpine fault, New Zealand: Geology, v. 40, no. 12, p. 1143-1146.

Townend, J., 1999, Heat flow through the West Coast, South Island, New Zealand: New Zealand Journal of Geology and Geophysics, v. 42, p. 21–31.

Townend, J., Sutherland, R., and Toy, V., 2009, Deep Fault Drilling Project—Alpine Fault, New Zealand: Scientific Drilling, v. 8, p. 75-82.

Townend, J., Sutherland, R., Toy, V., Eccles, J., Boulton, C., Cox, S., and McNamara, D., 2013, Late-interseismic state of a continental plate-bounding fault: Petrophysical results from DFDP-1 wireline logging and core analysis, Alpine Fault, New Zealand: Geochemistry, Geophysics, Geosystems, v. 14, no. 9, p. 3801-3820.

Toy, V. G., Boulton, C. J., Sutherland, R., Townend, J., Norris, R. J., Little, T. A., Prior, D. J., Mariani, E., Faulkner, D., Menzies, C. D., Scott, H., and Carpenter, B., 2015, Fault rock lithologies and architecture of the central Alpine fault, New Zealand, revealed by DFDP-1 drilling: Lithosphere, v. 7, no. 2, p. 155-173.

Toy, V. G., Sutherland, R., Townend, J., Allen, M. J., Becroft, L., Boles, A., Boulton, C., Carpenter, B., Cooper, A., and Cox, S. C., 2017, Bedrock geology of DFDP-2B, central Alpine Fault, New Zealand: New Zealand Journal of Geology and Geophysics, p. 1-22.